Elsevier Editorial System(tm) for Icarus
Manuscript Draft

Manuscript Number:

Title: Evidence for an Explosive Origin of Central Pit Craters on Mars

Article Type: Regular Article

Keywords: central pit crater; Mars; THEMIS

Corresponding Author: Mr. Nathan Robert Williams,

Corresponding Author's Institution: Arizona State University

First Author: Nathan Robert Williams

Order of Authors: Nathan Robert Williams; James F Bell; Philip R Christensen; Jack D Farmer

Abstract: Kilometer-scale pit craters are nested in the centers of many impact craters on Mars, as well as icy satellites. They have been inferred to form in the presence of a water-ice rich substrate; however, the process(es) responsible for their formation is still debated. Leading hypotheses invoke origins by either explosive excavation, or by subsurface drainage and collapse. If explosive excavation forms central pit craters, ejecta blankets should be draped around the pits, whereas internal collapse should not deposit significant material outside pit rims. Using visible wavelength images from the MRO CTX and HiRISE instruments and thermal infrared images from the Odyssey THEMIS instrument, we conducted a survey to characterize, in detail, the global population of central pits in impact craters ≥10 km in diameter. We specifically examined the morphology and thermophysical characteristics of the pits for evidence of ejecta blankets. We observed raised rims around many central pits, with morphologies similar to rims around impact craters and maar volcanoes. Our analysis of thermal images suggests that blocky materials - which we interpret as pit ejecta - are draped around many central pits on the floors of their parent craters. These observations and interpretations support an explosive origin for central pit craters on Mars. Theoretical calculations show that more than enough thermal energy is available via impact melt from the parent crater to form central pits by steam explosions, and such explosions would require only a modest amount (~3% by volume) of subsurface water-ice. We therefore propose that central pit craters on Mars could have formed explosively by the interaction of impact melt and subsurface water-ice.

Suggested Reviewers: Nadine Barlow
Nadine.Barlow@nau.edu
Previously published several papers regarding central pit craters.

Veronica Bray
vjbray@lpl.arizona.edu
Previously published on central pit craters

Devon Burr
dburr1@utk.edu
Previously published on evidence of Martian fluvial activity from satellite image analysis

Steve Clifford

clifford@lpi.usra.edu
Previously published work on Mars cryosphere and the role of ice in planetary regoliths

Christopher Edwards
cedwards@caltech.edu
Previously published on using THEMIS data to infer/determine thermal inertia and block abundance

Catherine Elder
cmelder@lpl.arizona.edu
Previously published on central pit craters

Robin Fergason
rfergason@usgs.gov
Previously published on using THEMIS data to infer/determine thermal inertia

Alfred McEwen
mcewen@lpl.arizona.edu
Previously published on using thermal data to identify impact crater ejecta, as well as discovering recurring slope lineae that may indicate present-day subsurface water seeps.

Jay Melosh
jmelosh@purdue.edu
Has published extensively on impact cratering

Peter Schultz
Peter_Schultz@brown.edu
Has published extensively on impact cratering

Livio Tornabene
ltornabe@uwo.ca
Previously published on using thermal data to identify impact crater ejecta

Opposed Reviewers:

To the Icarus editorial board:

We are submitting the manuscript entitled “Evidence for an Explosive Origin of Central Pit Craters on Mars” for your consideration. In this manuscript, we report the results of our survey of central pit craters on Mars using THEMIS thermal images. We use these images to identify blocky material around the pits to test hypotheses of pit formation by explosion excavation, or drainage and collapse.

Assessing the distribution and history of water is a key issue in Martian science. Over several hundred central pit craters are found on Mars as well as icy satellites, but rarely other rocky planets, and are therefore inferred to form in the presence of water. Our interpretation of central pits as explosive craters requires much less water than drainage and collapse models that suggested unrealistically large volumes of water in the subsurface at low- and mid-latitudes.

Our results are notable for many reasons, including:

(1) Blocky debris and raised rims are common around central pit craters, suggestive of explosively-derived ejecta.

(2) The abundance of blocks distributed around central pit craters is not expected for collapse origin hypotheses.

(3) Only ~3% water by volume is required for explosive excavation of central pit-scale craters on Mars.

We believe that our study will be of interest to the Icarus readership because it provides new thermal imaging observations to test and distinguish between the primary origin hypotheses for central pit craters.

This is our first attempt at submission of this manuscript. We suggest possible reviewers might include:
Nadine Barlow (Nadine.Barlow@nau.edu), Veronica Bray (vjbray@lpl.arizona.edu), Devon Burr (dburr1@utk.edu), Steve Clifford (clifford@lpi.usra.edu), Christopher Edwards (cedwards@caltech.edu), Catherine Elder (cmelder@lpl.arizona.edu), Robin Fergason (rfergason@usgs.gov), Alfred McEwen (mcewen@lpl.arizona.edu), Jay Melosh (jmelosh@purdue.edu), Pete Schultz (Peter_Schultz@brown.edu), Livio Tornabene (ltornabe@uwo.ca).

We look forward to your response.

Sincerely,

Nathan Williams
Geological Sciences Ph.D. Candidate
School of Earth and Space Exploration

Arizona State University

ISTB-4, Room 631
Arizona State University
781 E. Terrace Road
Tempe, AZ 85287-6004

Nathan.R.Williams@asu.edu
413-695-9896

*Manuscript
Click here to view linked References

Evidence for an Explosive Origin of Central Pit Craters on Mars

Nathan R. Williams[1], James F. Bell III[1], Philip R. Christensen[1], Jack D. Farmer[1]

[1]School of Earth and Space Exploration, Arizona State University, Tempe, AZ, USA

Abstract:

Kilometer-scale pit craters are nested in the centers of many impact craters on Mars, as well as icy satellites. They have been inferred to form in the presence of a water-ice rich substrate; however, the process(es) responsible for their formation is still debated. Leading hypotheses invoke origins by either explosive excavation, or by subsurface drainage and collapse. If explosive excavation forms central pit craters, ejecta blankets should be draped around the pits, whereas internal collapse should not deposit significant material outside pit rims. Using visible wavelength images from the MRO CTX and HiRISE instruments and thermal infrared images from the Odyssey THEMIS instrument, we conducted a survey to characterize, in detail, the global population of central pits in impact craters ≥10 km in diameter. We specifically examined the morphology and thermophysical characteristics of the pits for evidence of ejecta blankets. We observed raised rims around many central pits, with morphologies similar to rims around impact craters and maar volcanoes. Our analysis of thermal images suggests that blocky materials – which we interpret as pit ejecta – are draped around many central pits on the floors of their parent craters. These observations and interpretations support an explosive origin for central pit craters on Mars. Theoretical calculations show that more than enough thermal energy is available via impact melt from the parent crater to form central pits by steam explosions, and such explosions would require only a modest amount (~3% by volume) of

subsurface water-ice. We therefore propose that central pit craters on Mars could have formed explosively by the interaction of impact melt and subsurface water-ice.

Introduction:

Central pit craters occur in many impact structures on Mars and exhibit a crater-in-crater configuration [Smith, 1976; Hodges, 1978; Barlow, 2011] (Fig. 1). Over one thousand pit craters have been identified on the floors, or on top of the central peaks of Martian impact craters with diameters between 5 and 114 km, with 75% being in impact craters with diameters between 7 and 30 km [Smith, 1976; Barlow, 2011]. Central pits have typical diameters of ~20% of the entire impact structure, such that a 50 km diameter crater might have a central pit ~10 km wide [Hodges, 1978]. Their depths range from very shallow, to over 1.5 km below the surrounding impact crater floor.

Central pit craters on Mars are confined to low and mid-latitudes, within ±70° of the Martian equator [Hodges, 1980; Barlow, 2011]. Central pits are also common for impact craters on icy satellites, including Ganymede and Callisto [Smith et al., 1979]. Central pits are seldom observed on rocky planets other than Mars, although a few dozen are present on Mercury [Schultz, 1989; Xiao and Komatsu, 2013] and the Moon [Croft, 1981; Schultz, 1976a, 1976b, 1988; Xiao *et al*., 2014].

The presence of water-ice is believed to be involved in typical pit crater formation [Hodges, 1980; Croft, 1981]. Although water-ice is not stable on low-latitude Martian surfaces today [Clifford and Hillel, 1983; Mellon *et al*., 1997; Head *et al*., 2003], water was (and might still be) present within the upper few kilometers of the surface even at low latitudes earlier in Mars' history. The possibility of significant subsurface water in pre-impact terrains is supported

by the presence of lobed ejecta surrounding many Martian rampart impact craters [Carr *et al*., 1977; Gault and Greeley, 1978; Wohletz and Sheridan, 1983; Barlow *et al*., 2000; Baloga *et al*., 2005], channels/deposits from catastrophic floods [Baker and Milton, 1974, Carr, 1979; Baker, 1982; McKenzie and Nimmo, 1999; Burr *et al*., 2002; Peel and Fassett, 2013], recent gullies [Christensen, 2003; McEwen *et al*., 2011], and Mars Odyssey Gamma Ray Spectrometer spectra [Boynton *et al*., 2007]. However, the process(es) responsible for forming central pits in craters and the role of water is still debated.

Two basic models have been proposed for pit formation: explosive excavation during, or after impact [Wood *et al*., 1978; Hodges, 1978; Hodges *et al*., 1980; Greeley *et al*., 1982; Barlow, 2006, 2010], or post-impact drainage and/or collapse [Croft, 1981; Passey and Shoemaker, 1982; Barlow, 2011; Alzate and Barlow, 2011; Elder *et al*., 2012; Bray *et al*., 2012]. Explosive excavation could be accomplished through vaporization of water/ice, such that thermal energy may be converted to kinetic, as pressurized steam expands rapidly, catastrophically excavating crater materials. Vaporization could occur from the heat and pressure of the parent crater-forming impact, or by later contact and mixing of impact rock-melt with water initiating a phreatomagmatic explosion. Low-velocity impacts have also been proposed as a possible explosive origin for central pits [Schultz, 1988]. The lack of infilling of central pits suggests that they formed late in or after the modification stage of the parent impact crater formation [*e.g.* Melosh, 1989]. Therefore, pit formation by immediate vaporization, or directly by impact excavation, is not favored. Alternatively, an icy substrate could be fractured and melted or sublimated during an impact, allowing water to either escape into the atmosphere, or drain gravitationally to deeper open pore space, leaving emptied pore space prone to collapse [Croft, 1981].

During a crater-forming explosion, rocks and boulders are ejected out of the crater, layers are proximally uplifted and overturned, and ejecta is draped over the surrounding surface to create raised rims [*e.g.* Melosh, 1989]. Features such as sinkholes , which are typical of karst landscapes, and lava tube skylights form by gravitational collapse and do not create raised rims by ejecting large quantities of material [*e.g.*, Okubo and Martel, 1998; Salvati and Sasowsky, 2002; Cushing *et al*., 2007; Robinson *et al*., 2012]. We hypothesize, then, that the presence or absence of an ejecta blanket provides one way to distinguish between explosive versus collapse scenarios for the formation of central pit craters. In this paper, we provide a summary of the data and methods used to test this hypothesis. Next, we examine the plausibility of enough thermal energy in a post-impact environment for initiating and sustaining steam explosions that could create kilometer-scale central pit craters. Finally, we apply our integrated observations to interpret the morphology and thermal properties of central pit craters.

Data and Methods:

For this study, we surveyed and identified impact craters > ~10 km in diameter containing central pits, within ±60° latitude of the Martian equator; surveys utilized the Java-based planetary geographic information system program JMARS [Christensen *et al*., 2009]. Central pit craters were identified as distinctive circular depressions in the center of an impact crater that appeared to be deeper than the parent crater floor based on the available imaging and topography. Diameters were measured for both the central pits and their parent craters. Many central pit craters were too small to identify or measure in the 128 pixel/deg (460 m/px) Mars Orbiter Laser Altimeter (MOLA) global shaded relief mosaic [Smith *et al*., 2001], so the ~100 m/pixel Mars Odyssey mission Thermal Emission Imaging Spectrometer (THEMIS)

[Christensen *et al*., 2004] calibrated daytime infrared (IR) global mosaic [Edwards *et al*., 2011] was used instead, which provides nearly complete coverage to ±60° latitude. THEMIS daytime IR images show topography as shaded relief, since Sun-facing slopes are typically warmest. Higher resolution images were also used to observe finer-scale morphology. Mars Reconnaissance Orbiter mission Context Camera (CTX) [Malin *et al*., 2007; Bell *et al*., 2013] images at ~ 6 m/pixel were map-projected and stretched from Planetary Data System (PDS) raw electronic data records, and High Resolution Imaging Science Experiment (HiRISE) [McEwen *et al*., 2007] images at ~ 0.25 to 1.3 m/pixel were map-projected and stretched from PDS calibrated reduced data records.

During the formation of impact and other explosive craters, large blocks are typically ejected and scattered outside the crater. Large blocks and coarse grains have higher thermal inertia than finer-grained materials and hold onto their heat longer through the night. The THEMIS nighttime thermal image mosaic can therefore be used as a proxy for blockiness, such that coarse-grained, or blocky materials are relatively warm while dust, sand, and other fine-grained materials are cooler [Christensen, 1986; Fergason *et al*., 2006; Edwards *et al*., 2009; Edwards *et al*., 2011]. THEMIS nighttime images have previously been used to observe blocky ejecta rays from impact craters on Mars that otherwise show little or no albedo variation in visible images [McEwen *et al*., 2005; Tornabene *et al*., 2006]. Similarly, central pit craters with an annulus, or a skewed patch of material that is relatively warmer in the THEMIS nighttime mosaic than the surrounding parent crater floor, can be classified as blocky (perhaps ejecta). Regional albedos around pits were also measured using Thermal Emission Spectrometer (TES) solar energy reflectivity integrated from 0.3 to 2.9 μm [Christensen *et al*., 2001].

Theoretical Modeling:

We also explored the theoretical plausibility of whether enough thermal energy could have been available in a post-impact environment to initiate steam explosions capable of creating kilometer-scale central pit craters. We started with the empirical model shown below which predicts the mass ratio of melted (m_m) to displaced (m_d) impact target materials (Eq. 1) [O'Keefe and Ahrens, 1982]:

$$m_m/m_d=1.6\times10^{-7}\times(g\times D_i)^{0.83}\times v_i^{0.33} \quad (1),$$

where g is planetary gravity, D_i is parent crater diameter and v_i is bolide velocity. We assign the following values for our calculations: Gravity g = 3.711 m/s^2; bolide velocity v_i = 25 km/s; central pit to parent crater diameter ratio = 0.2, and depth/diameter ratio for the parent crater = 0.1. We also assumed that any melt generated remained within the crater. Finally, we modeled the crater as a half-ellipsoid and applied the mass fraction to determine the volume and mass of melt produced (Eqs. 2,3):

$$V_m=(m_m/m_d)\times(2/3)\times\pi\times d_i\times(D_i/2)^2 \quad (2) \text{ and}$$

$$m_m=\rho_m/V_m \quad (3),$$

where V_m is the volume of melt, d_i is the depth of the parent crater, and ρ_m is the density of the melt. Sato and Taniguchi (1997) used the following equation to predict the energy required to form (in this case, a central pit) crater, explosively. The empirical equation can be applied to volcanic, nuclear, and chemical explosions, independent of origin (Eq. 4):

$$E_c=4.45\times10^6\times D_p^{3.05} \quad (4),$$

where E_c is the energy of crater formation and D_p is the diameter of the (pit) crater. The total thermal energy transfer required to melt ice and boil water to steam can be calculated using specific and latent heats (Eq. 5):

$$H_w = m_w \times L_f + m_w \times c_{lq} \times \Delta T_w + m_w \times L_v \quad (5),$$

where H_w is the energy transferred to the water, m_w is the mass of water, L_f is the latent heat of fusion, c_{lq} is the specific heat of liquid water, ΔT_w is the temperature change of liquid water, and L_v is the latent heat of vaporization. We assign values for L_f = 3.34x10^5 J/kg, c_{lq} = 4.187 x10^3 J/kg·K, and L_v = 2.270 x10^6 J/kg. Evaluating Eq. 5, we see that an investment of 3.023x10^6 J is required to turn 1 kg of water from ice (273 K) to steam (373 K). We assume that the steam is not heated to higher temperatures, although a smaller amount of superheated steam would also satisfy the energy requirements for crater formation. The thermal energy of vaporization, specifically the step of converting water to steam, can be transformed to kinetic energy that can form a crater. The mass of steam required is calculated by dividing the crater formation energy from Eq. 4 by the latent heat of vaporization. Dividing this result by the density of ice provides the volume of ice required to form a central pit crater. As shown in Fig. 2, only a small amount of water (comprising ~3% of a central pit's volume) would need to be vaporized to form a central pit crater.

The amount of thermal energy available in rock-melt may also be calculated using specific heats (Eq. 6):

$$E_m = m_m \times c_{pm} \times \Delta T_m = \rho_m \times V_m \times c_{pm} \times \Delta T_m \quad (6),$$

where E_m is the energy required for cooling rock, c_{pm} is the specific heat of rock, ΔT_m is the temperature change of the rock. We assume a basaltic melt composition and assign values of ρ_m = 3000 kg/m^3; c_{pm} = 1000 J/kg·K; and change of temperature (from the basalt solidus to the STP boiling point of water) ΔT_m = 1473 K – 373 K = 1100 K. It should be noted that impact melts can also be superheated, perhaps up to 1700°C (1973 K) [Zieg and Marsh, 2005], so our calculations may underestimate the thermal energy available by ~50%. Adiabatic heat transfer efficiency is

typically ~10% or less, due to poor mixing; however, it can reach an optimal efficiency of ~30% for water/melt ratios of 0.3-0.5 [Wohletz, 1986]. Such optimal efficiencies are believed to be present for maars in permafrost, as suggested by the largest, kilometer-scale terrestrial maars found in the Seward Peninsula, Alaska [Begét *et al*., 1996]. Our calculations consider cases with both 10% (suboptimal) and 30% (optimal) efficiencies.

The mass of impact melt required to vaporize ice to steam can be calculated by setting the total heat transfer H_w from Eq. 5 equal to the product of the heat transfer efficiency and the rock-melt thermal energy from Eq. 6. As shown in Fig. 2, the rock-melt must comprise a volume greater than or equal to ~8-28% of the central pit crater's volume. The total energy transfer required for vaporizing ice (H_w) from Eq. 5 can also be compared to the total energy available from rock-melt by multiplying Eq. 6 with the value(s) for heat transfer efficiency (Figs. 3, 4). Based on these calculations, sufficient thermal energy should be available via impact rock-melt to vaporize small amounts of ice that act explosively to form central pit craters within kilometer-scale impact structures.

Results:

We identified central pit craters within 654 parent craters ~10 km diameter or larger between ±60° latitude of the Martian equator (Fig. 5). Additional smaller craters with central pits likely exist, but are not resolved in THEMIS thermal images used for this study. Topographic profiles across many of the larger central pit craters show raised rims around central pits that taper outwards (Fig. 5). Central pits were identified in parent impact craters with diameters from ~8 to 112 km, with 95% of those parent craters being less than 50 km in diameter. Some impact craters with diameters <10 km containing central depressions were excluded from our survey due

to poor spatial resolution and uncertainty as to whether the depressions were deeper than the parent floor. We excluded ambiguous structures that might be peak rings or concentric terraces, especially in craters near the Martian simple to complex crater transition of ~3-8 km diameter [Pike, 1980]. The surveyed central pits have a median diameter ratio to their parent craters of 0.175 with a standard deviation of 0.037 (Fig. 6). These results are comparable to the median ratio of 0.16 found by Barlow [2011].

Based on THEMIS nighttime temperature images, 388 (59.3%) pits showed warm (coarse) material outside their rim and on the parent crater floor (Fig. 7); the remaining 266 (40.7%) did not. Some pits had annuli of warm material surrounding the whole pit, whereas others showed increased nighttime temperatures on predominantly one side (Fig. 8). Pits with warm patches in THEMIS images showed large blocky debris (up to tens, to perhaps over a hundreds of meters wide for the largest pits) in visible CTX and HiRISE images (Fig. 9), while pits that did not show warm material typically appeared blanketed or mantled by sand and/or dust (Fig. 10).

Based on TES-derived albedos, central pits in Tharsis, Elysium, Arabia, and other high-albedo (dusty) regions tend to not be surrounded by warm material (Figs. 4, 11). The median albedo for all central pits with warm material is 0.16, while the median albedo for all central pits without is 0.23. However, the albedo distribution on Mars is bimodal, due to regional dust deposits, so we also examined the medians separately for dusty (albedo >0.19), versus non-dusty areas (albedo <0.19). In non-dusty areas, 254 pits (70%) have warm material versus 106 (30%) that do not. As expected, the median albedo around pits within non-dusty areas was the same (0.14) for pits both with and without warm material. Conversely in regions with albedos > 0.19, dust significantly affects the detection of warm, blocky material. There are fewer (134, 46%) pits

with warm material in dusty regions with a medial albedo of 0.236, while pits without warm material (160, 54%) had a median albedo of 0.267. Therefore, pits in non-dusty areas are more likely to show warm material. We conclude that dust plays a significant role in the masking blocky material around many central pits.

Smaller central pits also tend to lack warm, blocky material (Fig. 12). Based on the population of impact craters observed with THEMIS data, the median diameter for parent craters containing pits with warm material is ~23.9 km and the median diameter for craters with pits lacking it is ~16.9 km, both cases being above the simple/complex transition of 3-8 km for Martian craters [Pike, 1980].

Discussion:

The raised rims around some pits observed with MOLA topography are suggestive of explosive excavation, similar to their parent craters, which also have raised rims. Surfaces visible in CTX and HiRISE images show large (meter-scale) blocks in warm patches adjacent to central pits (*e.g.*, Fig. 9), consistent with the expected correlation between warm material and coarse surfaces. Such blocks and megablocks are commonly observed near explosively-formed craters, including at the Ries crater in Germany [Gault *et al*., 1963], as well as at some Martian craters [*e.g.*, Caudill *et al*., 2012]. Combined with the spatial correlation of warm material and central pits, we interpret the blocks scattered around central pits to be explosively-emplaced pit ejecta.

Central pit craters appear to be eroded and degraded in a similar manner to their parent craters, suggesting that the pits formed relatively soon after the parent impacts. The presence or absence of warm, coarse-grained materials appears to depend on the degradational state of the pit and its parent crater. Small craters excavate a smaller volume of material that is finer-grained on

average [Gault *et al*., 1963] and may be more easily eroded, or covered than large craters. The more frequent and larger ejecta blocks at larger pits, however, should be preferentially preserved and exposed at or within a few thermal skin depths (several centimeters) of the surface. Accumulated dust and/or sand appears to mask ejecta, as indicated by typically higher albedos and/or the blanketed appearance for pits lacking warm material (Fig. 11). The positive correlation of albedo and pit crater diameter suggests that the thermal anomalies of smaller pit craters are often masked by degradation and/or burial.

Taken out of context, the presence of warm material near pits would not necessarily need to be due to ejecta. For example, post-impact lava or perhaps impact melt flows occur near a few pits and also have high thermal inertias, although small flow lobes are easily distinguishable and more extensive volcanism should have filled the central pit (Fig. 13). Patchy or partial erosional uncovering of consolidated parent crater fill rocks could also explain higher thermal inertias relative to the surrounding crater floor; however, the unlikely selective removal of significant amounts of dust from the centers of parent craters, but not in the dusty plains surrounding many parent craters, argues against such a mechanism. Additionally, significant erosion on the parent crater floor is inconsistent with the presence and preservation of raised rims around many central pits. The high thermal inertia signals are also not associated with any aeolian dunes or other bedforms, based on CTX and HiRISE images.

Our calculations suggest that rock-melt from kilometer-scale impacts has sufficient thermal energy to drive steam explosions capable of producing pit craters; however, not all Martian craters exhibit central pits. We propose two primary criteria for the explosive formation of central pits on Mars: the coexistence of impact generated rock-melt and water-ice. First, sufficient impact melt must be retained within the parent impact crater. Smaller impact craters

produce less melt proportionally and distribute that impact melt more sparsely, so small craters may not have enough consolidated rock-melt energy to ultimately form pits, even if sufficient water-ice is present. Additionally, if the system has excess water-ice, the rock-melt's thermal energy may also melt and heat the excess water and not have sufficient energy remaining to vaporize enough water to form a pit crater. Second, sufficient water must be available post-impact. If too little water (or too low a concentration) is present, there may not be sufficient steam to form a large pit crater. Although only a small amount (~3% by volume) of water is required to drive a pit-forming steam explosion, larger impact craters (tens to hundreds of km) may produce enough rock-melt to fill in any depressions that might form and thus erase any topographic evidence of a central pit. A similar phenomenon is thought to have occurred at the Sudbury impact structure, where steam explosions created the brecciated Onaping Formation but the explosive depressions were filled in and erased [Grieve *et al*., 2010].

Contact and interaction of impact rock-melt and water/ice could be accomplished through several mechanisms. For example, heavy fracturing and brecciation during the impact process may allow fluids (either rock-melt, or liquid water) to mobilize and permeate the substrate and come into contact with each other. Water (liquid), or ice-bearing fallback ejecta could also be deposited on top of impact rock-melt pools, or suevite deposits. However, these two mechanisms (as well as many collapse scenarios) would not necessarily require that pit craters always form in the centers of their parent craters, nor that they be consistently sized, because fracturing and fallback of ejecta should be ubiquitous over the crater interior and pore water volumes are likely to be spatially variable.

We propose an alternate hypothesis in which that the central uplift will sometimes bring sufficient water (as liquid, ice, or both) up and into contact with near-surface impact rock-melt to

initiate late impact-stage steam explosions that form central pit craters (Fig. 14). Central uplift occurs late in the impact process during the modification stage, after most crater fill has settled [*e.g.*, Melosh, 1989]. Thus, pit formation concurrent with central uplift is consistent with the apparent lack of infilling of deep pits. This model also explains why these large pits are always in the centers of their parent craters (where the central uplift occurred) and have raised rims and blocky materials (explosive ejecta) surrounding the pit craters. Another interesting aspect of this model is that since our calculations show it only requires small amounts of water (perhaps as little as 3% by volume), it provides a possible explanation even for the formation of the small number of central pit craters observed on Mercury and the Moon, which should have had very limited water, or other volatiles to sustain collapse. Although not directly addressed in our survey, smaller "summit pit craters" are also observed atop some Martian central peaks [Barlow, 2006, 2011], and can potentially be explained by this uplift contact model, representing cases where either water, or rock-melt is limited and localized.

Summary

The presence of raised rims and blocky material surrounding Martian central pit craters is consistent with ejecta from an explosive pit origin. Nearly 60% of all central pits in our global survey have relatively warmer (interpreted as coarser) material around them. Pits in areas with high albedos (dusty) tend to not show blocky materials, which have probably been obscured by dust accumulation. Smaller pits also tend not to show blocky material, perhaps because the less voluminous ejecta was finer-grained and more easily removed by erosion. Drainage and collapse models do not satisfactorily explain the observed characteristics of these features; for example, those processes are unlikely to emplace or concentrate blocky ejecta, as coarse materials should

move down slope, and not be preferentially concentrated on the rim. We propose a new "uplift contact model" that could explain the observed morphologies, distributions, and thermal properties of Martian central pit craters. Our thermal calculations show that only ≥ ~3% water by volume is required to provide the energy needed for a phreatomagmatic explosion origin for the observed pit craters. Our explosive origin model is also potentially consistent with the small number of central pits on Mercury and the Moon, assuming only minor amounts of water in localized pre-impact subsurfaces. Drainage and collapse may still be a viable method for pit formation on icy satellites, but an explosive origin for central pit craters appears to be the preferred mechanism for Mars (and other rocky planets) for forming central pit craters.

References:

Alzate, N., Barlow, N.G., 2011. Central pit craters on Ganymede. Icarus 211, 1274-1283.

Baker, V.R., 1982. The Channels of Mars. University of Texas Press. Austin. 198 pp.

Baker, V.R., Milton, D.J., 1974. Erosion by Catastrophic Floods on Mars and Earth. Icarus 23, 27-41.

Baloga, S.M., Fagents, S.A., Mouginis-Mark, P.J., 2005. Emplacement of Martian Rampart Crater Deposits. J. Geophys. Res. 110, E10001. doi:10.1029/2004JE002338.

Barlow, N.G., 2006. Impact Craters in the Northern Hemisphere of Mars: Layered Ejecta and Central Pit Characteristics. Met. & Planet. Sci. 41, 1425-1436.

Barlow, N.G., 2010. Central pit craters: Observations from Mars and Ganymede and implications for formation models. GSA Special Papers 465, 15-27.

Barlow, N.G., Boyce, J.M., Costard, F.M., Craddock, R.A., Garvin, J.B., Sakimoto, S.E.H., Kuzmin, R.O., Roddy, D.J., 2000. Standardizing the Nomenclature of Martian Impact Crater Ejecta Morphologies. J. Geophys. Res. 105, E11, 26733-26738.

Barlow, N.G., 2011. Constraints on the Proposed Formation Models for Martian Central Pit Craters. Lunar Planet. Sci. 42. Abstract #1149.

Begét, J.E., Hopkins, D.M., Charron, S.D., 1996. The Largest Known Maars on Earth, Seward Peninsula, Northwest Alaska. Arctic 49, 1, 62-69.

Bell, J.F., III, Malin, M.C., Caplinger, M.A., Fahle, J., Wolff, M.J., Cantor, B.A., James, P.B., Ghaemi, T., Posiolova, L.V., Ravine, M.A., Supulver, K.D., Calvin, W.M., Clancy, R.T., Edgett, K.S., Edwards, L.J., Haberle, R.M., Hale, A., Lee, S.W., Rice, M.S., Thomas, P.C., Williams, R.M.E., 2013. Calibration and Performance of the Mars Reconnaissance Orbiter Context Camera (CTX). Mars 8, 1-14. doi:10.1555/mars.2013.0001.

Boynton, W.V., Taylor, G.J., Evans, L.G., Reedy, R.C., Starr, R., Janes, D.M., Kerry, K.E., Drake, D.M., Kim, K.J., Williams, R.M.S., Crombie, M.K., Dohm, J.M., Baker, V.,

Metzger, A.E., Karunatillake, S., Keller, J.M., Newsom, H.E., Arnold, J.R., Bruckner, J., Englert, P.A.J., Gasnault, O., Sprague, A.L., Mitrofanov, I., Squyres, S.W., Trombka, J.I., d'Uston, L., Wanke, H., Hamara, D.K., 2007. Concentration of H, Si, Cl, K, Fe, and Th in the low- and mid-latitude regions of Mars. J. Geophys. Res. 112, E12S99. doi:10.1029/2007JE002887.Bray, V.J., Schenk, P.M., Melosh, H.J., Morgan, J.V., Collins, G.S., 2012. Ganymede crater dimensions – Implications for central peak and central pit formation and development. Icarus 217, 115-129.

Burr, D.M., McEwen, A.S., Sakimoto, S.E.H., 2002. Recent Aqueous Floods from the Cerberus Fossae, Mars. Geophys. Res. Let. 29, 1, 1013. doi: 10.1029/2001GL013345.

Carr, M.H., Crumpler, L.S., Cutts, J.A., Greeley, R., Guest, J.E., Masursky, H., 1977. Martian Impact Craters and Emplacement of Ejecta by Surface Flow. J. Geophys. Res. 82, 28, 4055-4065.

Carr, M.H., 1979. Formation of Martian Flood Features by Release of Water from Confined Aquifers. J. Geophys. Res. 84, B6, 2995-3007.

Christensen, P.R., 1986. The Spatial Distribution of Rocks on Mars. Icarus 68, 217-238.

Christensen, P.R., Bandfield, J.L., Hamilton, V.E., Ruff, S.W., Kieffer, H.H., Titus, T.N., Malin, M.C., Morris, R.V., Lane, M.D., Clark, R.L., Jakosky, B.M., Mellon, M.T., Pearl, J.C., Conrath, B.J., Smith, M.D., Clancy, R.T., Kuzmin, R.O., Roush, T., Mehall, G.L., Gorelick, N., Bender, K., Murray, K., Dason, S., Greene, E., Silverman, S., Greenfield, M., 2001. Mars Global Surveyor Thermal Emission Spectrometer experiment: Investigation description and surface science results. J. Geophys. Res. 106, E10, 23823–23871.

Christensen, P.R., 2003. Formation of Recent Martian Gullies through Melting of Extensive Water-rich Snow Deposits. Nature 422, 45-48.

Christensen, P.R., Engle, E., Anwar, S., Dickenshied, S., Noss, D., Gorelick, N., Weiss-Malik, M., 2009. JMARS – A Planetary GIS. http://adsabs.harvard.edu/abs/2009AGUFMIN22A..06C.

Christensen, P.R., Jakosky, B.M., Kieffer, H.H., Malin, M.C., McSween, H.Y., Jr., Nealson, K., Mehall, G.L., Silverman, S.H., Ferry, S., Caplinger, M., Ravine, M., 2004. The Thermal Emission Imaging System (THEMIS) for the Mars 2001 Odyssey Mission. Space Sci. Rev. 110, 85-130.

Clifford, S.M., Hillel, D., 1983. The Stability of Ground ice in the Equatorial Region of Mars. J. Geophys. Res. 88, B3, 2456-2474.

Croft, S.K., 1981. On the Origin of Pit Craters. Proc. Lunar Planet. Sci. Conf. 12, 196-198.

Cushing, G.E., Titus, T.N., Wynne, J.J., Christensen, P.R., 2007. THEMIS observes possible cave skylights on Mars. Geophys. Res. Let. 34, L17201. doi:10.1029/2007GL030709.

Edwards, C.S., Bandfield, J.L., Christensen, P.R., Fergason, R.L., 2009. Global Distribution of Bedrock Exposures on Mars using THEMIS High-resolution Thermal Inertia. J. Geophys. Res. 114, E11001. doi:10.1029/2009JE003363.

Edwards, C.S., Nowicki, K.J., Christensen, P.R., Hill, J., Gorelick, N., Murray, K., 2011. Mosaicking of global planetary image datasets: 1. Techniques and data processing for Thermal Emission Imaging System (THEMIS) multi-spectral data. J. Geophys. Res. 116, E10008. doi:10.1029/2010JE003755.

Elder, C.M., Bray, V.J., Melosh, H.J., 2012. Theoretical Plausibility of Central Pit Crater Formation Via Melt Drainage. Icarus 221, 831-843.

Fergason, R.L., Christensen, P.R., Kieffer, H.H., 2006. High Resolution Thermal Inertia Derived from THEMIS: Thermal Model and Applications. J. Geophys. Res. 111, E12004. doi:10.1029/2006JE002735.

French, B.M., 1998. Traces of Catastrophe. LPI Contribution No. 954, Lunar and Planet. Inst., Houston, Texas.

Gault, D.E., Greeley, R., 1978. Exploratory Experiments of Impact Craters Formed in Viscous-Liquid Targets: Analogs for Martian Rampart Craters?. Icarus 34, 486-495.

Greeley, R., Fink, J.H., Gault, D.E., Guest, J.E., 1982. Experimental simulation of impact cratering on icy satellites. In D. Morrison (Ed.), Satellites of Jupiter. University of Arizona Press, Tucson, Arizona. pp. 340-378.

Grieve, R.A.F., Ames, D.E., Morgan, J.V., Artemieva, N., 2010. The evolution of the Onaping Formation at the Sudbury impact structure. Met. Planet. Sci. 45, 5, 759-782.

Head, J. W., Mustard, J.F., Kreslavsky, M.A., Milliken, R.E., Marchant, D.R., 2003. Recent Ice Ages on Mars. Nature 426, 797-802.

Hodges, C.A., 1978. Central Pit Craters on Mars. Proc. Lunar Planet. Sci. Conf. 9, 521-522.

Hodges, C.A., Shew, N.B., Clow, G., 1980. Distribution of Central Pit Craters on Mars. Proc. Lunar Planet. Sci. Conf. 11, 450-452.

Malin, M.C., Bell, J.F., III, Cantor, B.A., Caplinger, M.A., Calvin, W.M., Clancy, R.T., Edgett, K.S., Edwards, L., Haberle, R.M., James, P.B., Lee, S.W., Ravine, M.A., Thomas, P.C., Wolff, M.J., 2007. Context Camera Investigation on board the Mars Reconnaissance Orbiter. J. Geophys. Res. 112, E05S04. doi:10.1029/2006JE002808.

McEwen, A.S., Preblich, B.S., Turtle, E.P., Artemieva, N.A., Golombek, M.P., Hurst, M., Kirk, R.L., Burr, D.M., Christensen, P.R., 2005. The rayed crater Zunil and interpretations of small impact craters on Mars. Icarus 176, 351-381.

McEwen, A.S., Eliason, E.M., Bergstrom, J.W., Bridges, N.T., Hansen, C.J., Delamere, W.A., Grant, J.A., Gulick, V.C., Herkenhoff, K.E., Keszthelyi, L., Kirk, R.L., Mellon, M.T., Squyres, S.W., Thomas, N., Weitz, C.M., 2007. Mars Reconnaissance Orbiter's High Resolution Imaging Science Experiment (HiRISE). J. Geophys. Res. 112, E05S02. doi:10.1029/2005JE002605.

McEwen, A.S., Ojha, L., Dundas, C.M., Mattson, S.S., Byrne, S., Wray, J.J., Cull, S.C., Murchie, S.L., Thomas, N., Gulick, V.C., 2011. Seasonal Flows on Warm Martian Slopes. Science 333, 740-743.

McKenzie, D., Nimmo, F., 1999. The Generation of Martian Floods by the Melting of Ground Ice Above Dikes. Nature 397, 231-233.

Mellon, M.T., Jakosky, B.M., Postawko, S.E., 1997. The Persistence of Equatorial Ground Ice on Mars. J. Geophys. Res. 102, E8, 19357-19369.

Melosh, H.J., 1989. Impact Cratering: A Geologic Process. Oxford Monographs on Geology and Geophysics #11, Oxford University Press, New York.

O'Keefe, J.D., Ahrens, T.J., 1985. Impact and Explosion Crater Ejecta, Fragment Size, and Velocity. Icarus 62, 328-338.

Okubo, C.H., Martel, S.J., 1998. Pit crater formation on Kilauea volcano, Hawaii. J. Volc. Geothermal Res. 86, 1-18.

Passey, Q.R., Shoemaker, E.M., 1982. Craters and basins on Ganymede and Callisto: Morphological indicators of crustal evolution. In: Morrison, D. (Ed.), Satellites of Jupiter. Univ. of Arizona Press, Tucson, Arizona. pp. 379-434.

Peel, S.E., Fassett, C.I., 2013. Valleys in pit craters on Mars: Characteristics, distribution, and formation mechanisms. Icarus 225, 272-282.

Robinson, M.S., Ashley, J.W., Boyd, A.K., Wagner, R.V., Speyerer, E.J., Hawke, B.R., Hiesinger, H., van der Bogert, C.H., 2012. Confirmation of sublunarean voids and thin layering in mare deposits. Planet. Space Sci. 69, 18-27.

Salvati, R., Sasowsky, I.D., 2002. Development of collapse sinkholes in areas of groundwater discharge. J. Hydrology 264, 1-11.

Sato, H., Taniguchi, H., 1997. Relationship Between Crater Size and Eject Volume of Recent Magmatic and Phreato-magmatic Eruptions: Implications for Energy Partitioning. Geophys. Res. Let. 24, 3, 205-208.

Schultz, P.H., 1976a. Floor-fractured lunar craters. Moon 15, 241-273.

Schultz, P.H., 1976b. Moon Morphology. University of Texas Press, Austin, Texas.

Schultz, P.H., 1988. Cratering on Mercury: A Relook. In: Villas, F., Chapman, C.R., Matthews, M.S. (Eds.), Mercury, University of Arizona Press, Tucson, Arizona, pp. 274-335.

Smith, E.I., 1976. Comparison of the Crater Morphology-Size Relationship for Mars, Moon, and Mercury. Icarus 28, 543-550.

Smith, B.A., Soderblom, L.A., Beebe, R., Boyce, J., Briggs, G., Carr, M., Collins, S.A., Cook, A.F., II, Danielson, G.E., Davies, M.E., Hunt, G.E., Ingersoll, A., Johnson, T.V., Masursky, H., McCauley, J., Morison, D., Owen, T., Sagan, C., Shoemaker, E.M., Strom, R., Suomi, V., Veverka, J., 1979. The Galilean Satellites and Jupiter: Voyager 2 Imaging Science Results. Science 206, 927-950.

Smith, D.E., Zuber, M.T., Frey, H.V., Garvin, J.B., Head, J.W., Muhleman, D.O., Pettengill, G.H., Phillips, R.J., Solomon, S.C., Zwally, H.J., Banerdt, W.B., Duxbury, T.C., Golombek, M.P., Lemoine, F.G., Newmann, G.A., Rowlands, D.D., Aharonson, O., Ford, P.G., Ivanov, A.B., Johnson, C.L., McGovern, P.J., Abshire, J.B., Afzal, R.S., Sun, X. 2001. Mars Orbiter Laser Altimeter: Experiment Summary After the First Year of Global Mapping of Mars. J. Geophys. Res. 106, E10, 23689-23722.

Tornabene, L.L., Moersch, J.E., McSween, H.Y., Jr., McEwen, A.S., Piatek, J.L., Milam, K.A., Christensen, P.R., 2006. Identification of large (2-10) km rayed craters on Mars in THEMIS thermal infrared images: Implications for possible Martian meteorite source regions. J. Geophys. Res. 111, E10006. doi:10.1029/2005JE002600.

Xiao, Z., Komatsu, G., 2013. Impact craters with ejecta flows and central pits on Mercury. Plan. Space Sci.. doi:10.1016/j.pss.2013.03.015.

Xiao, Z., Zeng, Z., Komatsu, G., 2014. A global inventory of central pit cratesr on the Moon: Distribution, morphology, and geometry. Icarus 227, 195-201.

Wohletz, K.H., Sheridan, M.F., 1983. Martian Rampart Crater Ejecta: Experiments and Analysis of Melt-Water Interaction. Icarus 56, 15-37.

Wohletz, K. H., 1986. Explosive Magma-water Interactions: Thermodynamics, Explosion Mechanics, and Field Studies. Bull. Volc. 48, 245-264.

Wood, C.A., Head, J.W., Cintala M.J., 1978. Interior Morphology of Fresh Martian Craters: The Effects of Target Characteristics. Proc. Lunar Planet. Sci. Conf. 9, 3691-3709.

Figures:

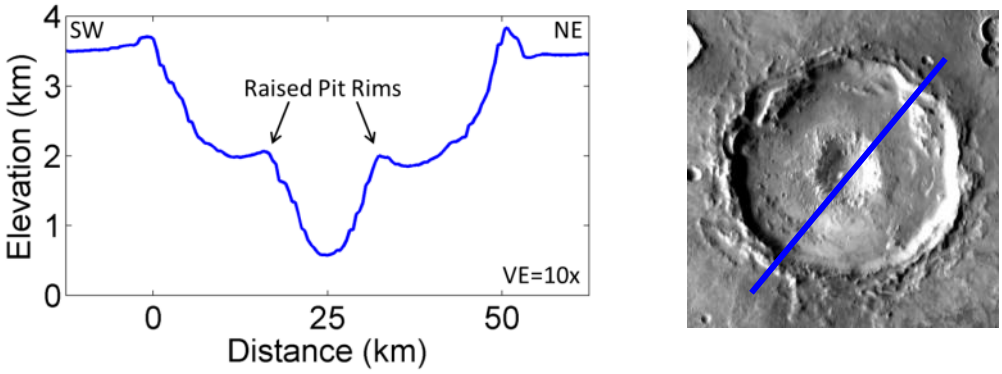

Fig. 1: MOLA topographic profile across the center of a 50 km diameter unnamed Martian impact crater containing a central pit at 296.4°E, 17.6°S (shown at right in THEMIS daytime mosaic). Note the raised rims on both the wider parent crater and the inner central pit. Vertical exaggeration is 10x.

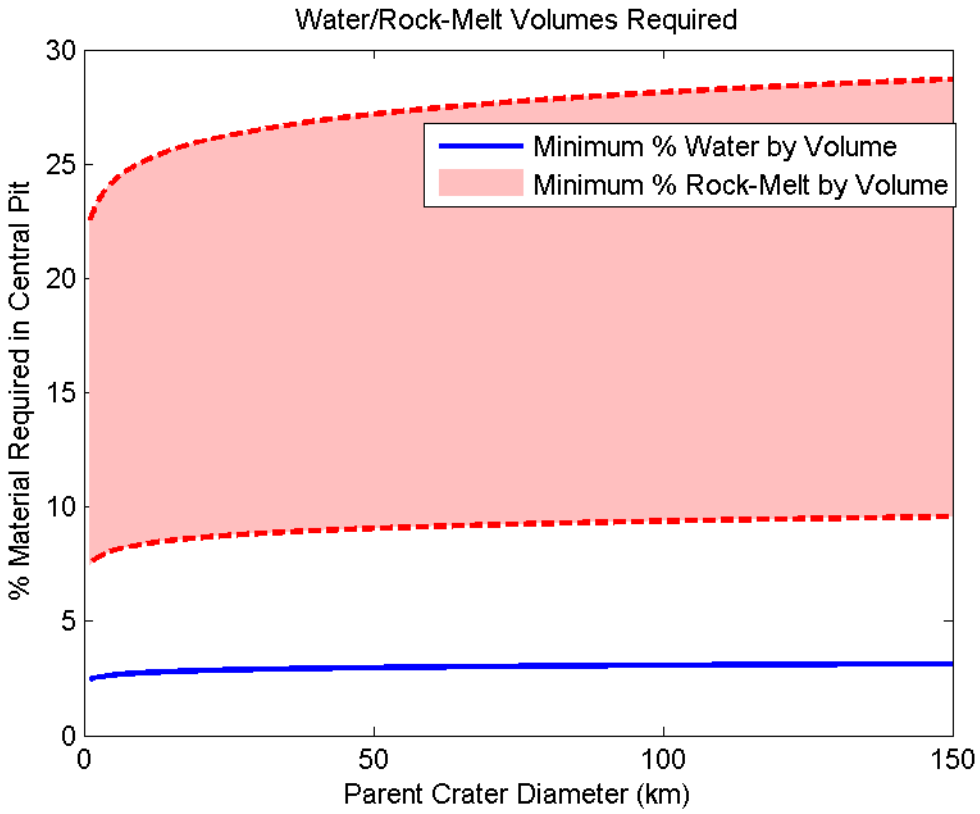

Fig. 2: Required amounts of water and impact melt for heat energy transfer to form a kilometer-scale (pit) crater shown as percent by volume with respect to the volume of a central pit crater. The range in impact melt volume represents uncertainty due to varying heat transfer efficiency between 0.1-0.3.

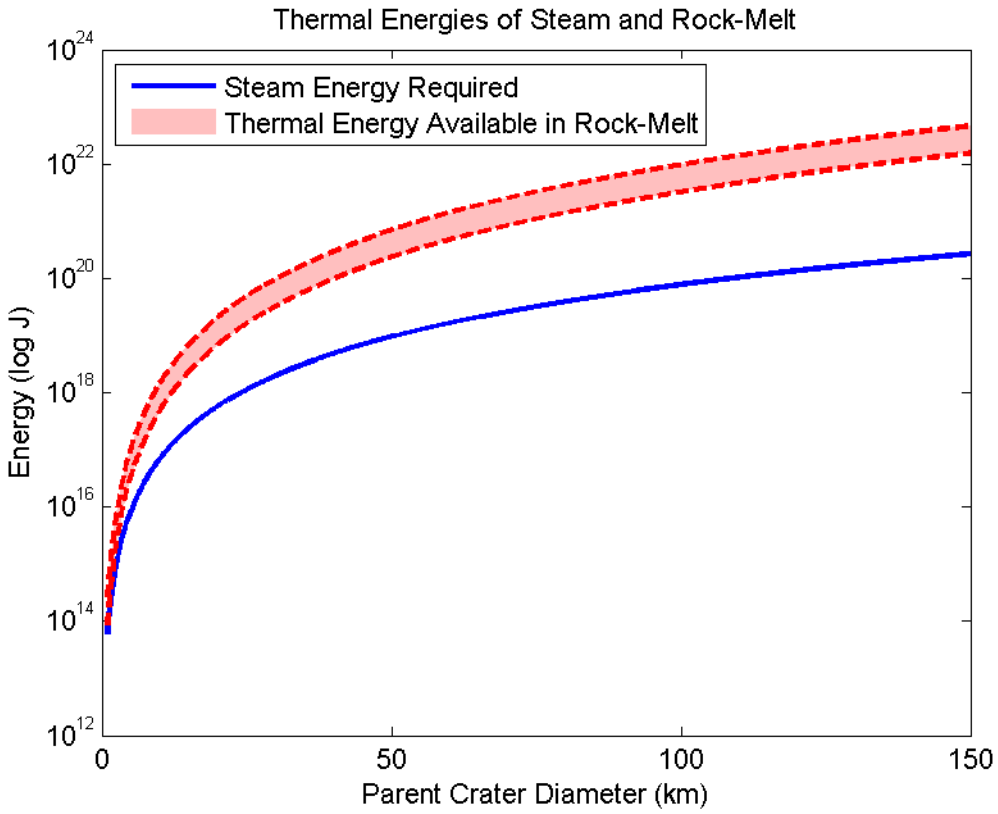

Fig. 3: Thermal energies of water required to convert ice to steam to provide the energy for creating central pit craters (blue line) of differing diameter. Also shown is the available thermal energy from impact rock-melt, after applying thermal efficiency values of 0.1 (lower red curve) to 0.3 (upper red curve).

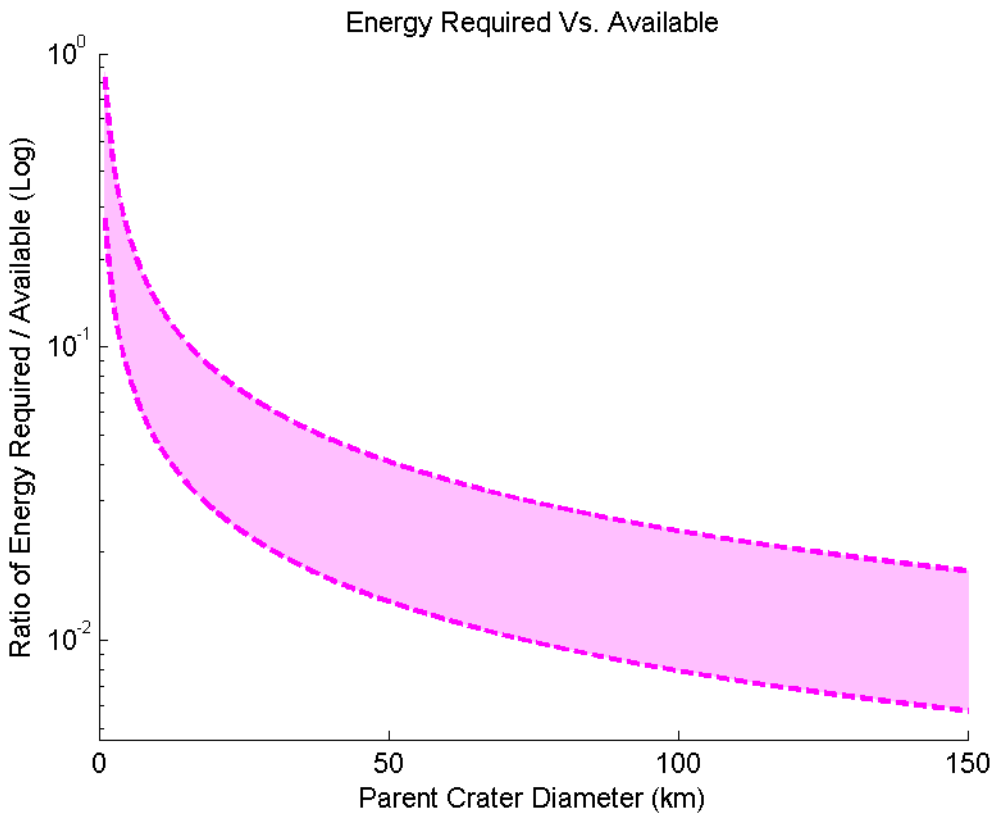

Fig. 4: Ratios of thermal energy required to vaporize steam, versus the amount of thermal energy available in relationship to crater diameter. The range of in energy ratios reflects variations in heat transfer efficiency over a range of 0.1 (lower curve) to 0.3 (upper curve).

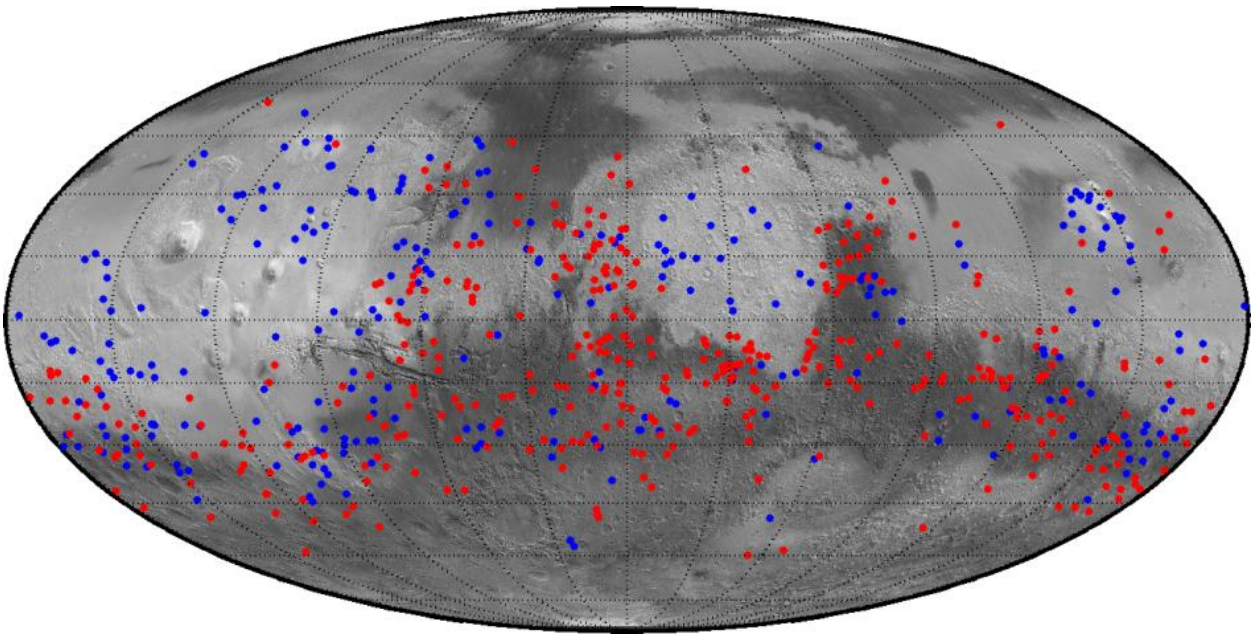

Fig. 5: Distribution of 654 central pit craters identified in our survey of the THEMIS daytime global mosaic, within ±60° degrees of the Martian equator, overlain on the TES albedo basemap [Christensen *et al*., 2001] and presented in a Mollweide equal area projection.

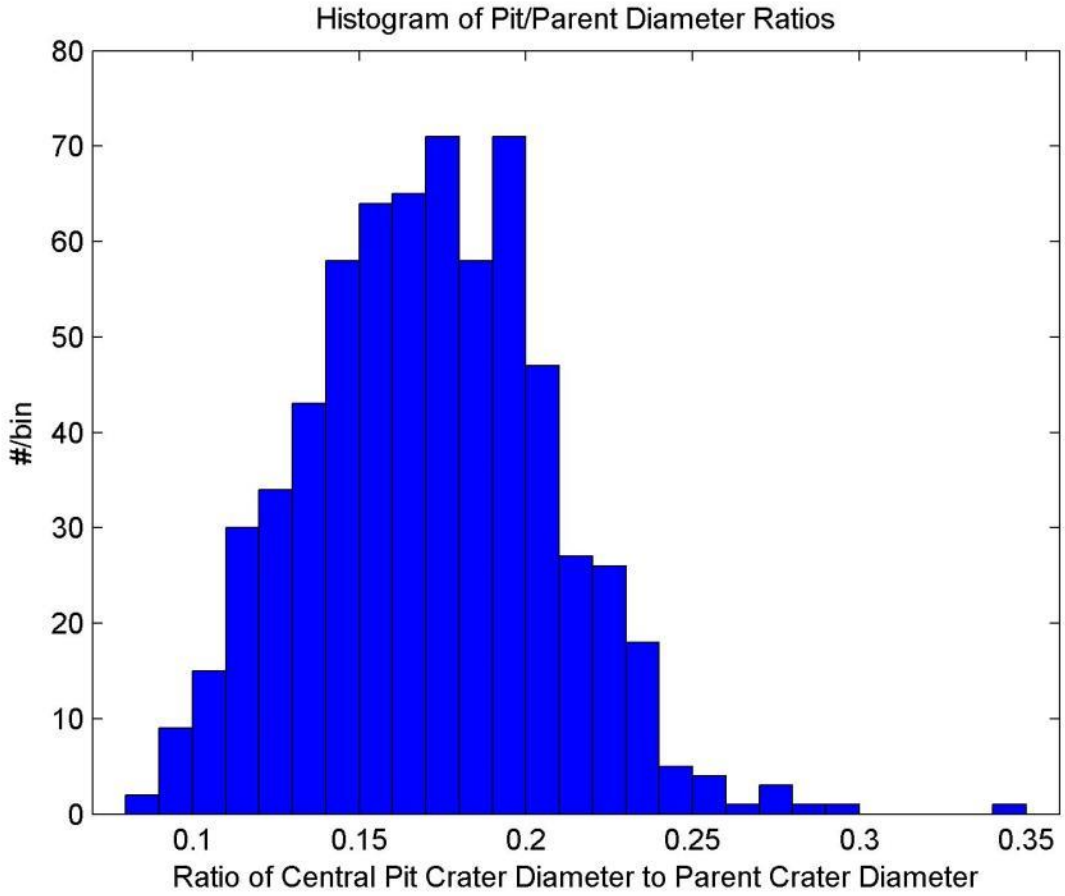

Fig. 6: Histogram showing the range of diameter ratios between central pits and their parent craters. The median value is 0.175 with a standard deviation of 0.037.

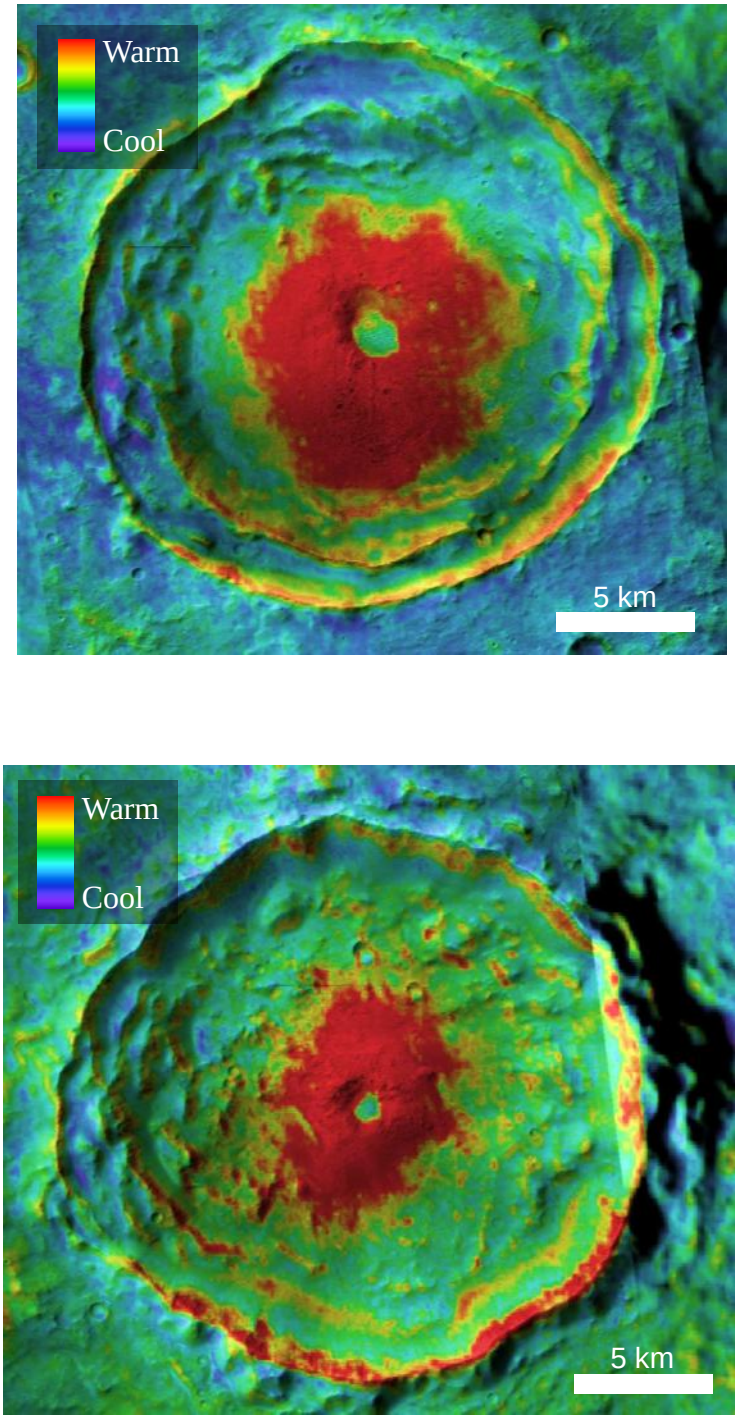

Fig. 7: CTX visible (shading) and THEMIS nighttime (color) images showing relatively warm material inferred to be blocky ejecta surrounding two central pit craters at 18.4°S, 102.7°E and 14.7°S, 93.2°E. The difference between "warm" and "cool" temperatures in these and other THEMIS nighttime IR images presented here is on the order of ~10K.

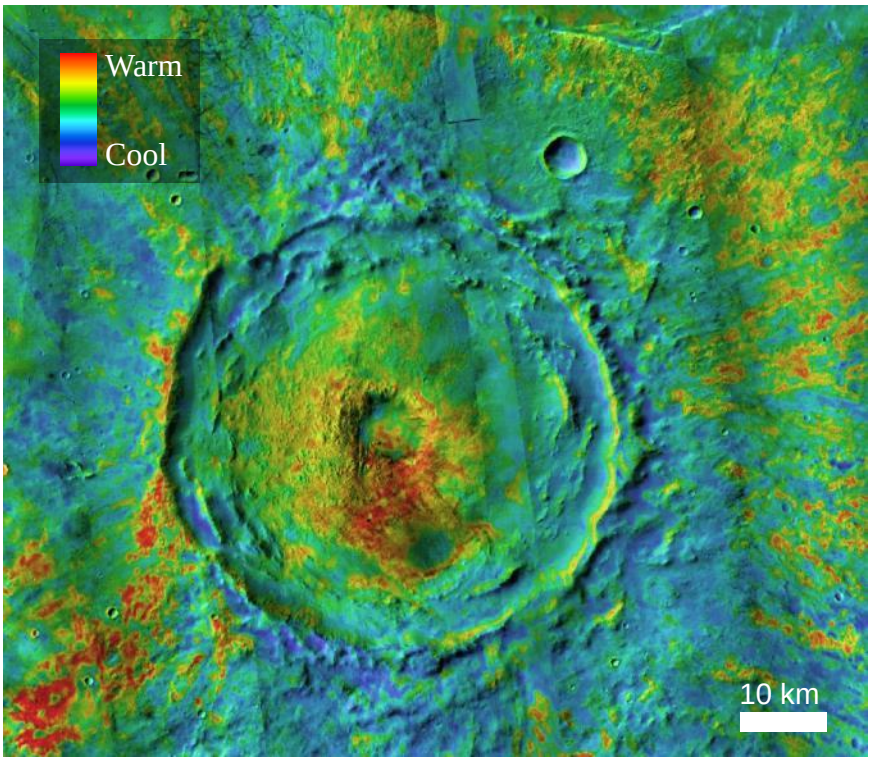

Fig. 8: THEMIS nighttime IR (color) over CTX visible (shading) image showing Arima crater (15.8°S, 296.3°E) and central pit with warm (blocky) material predominantly on the south and west sides. Note the parent crater's distal ejecta is also warm, indicating blocky debris.

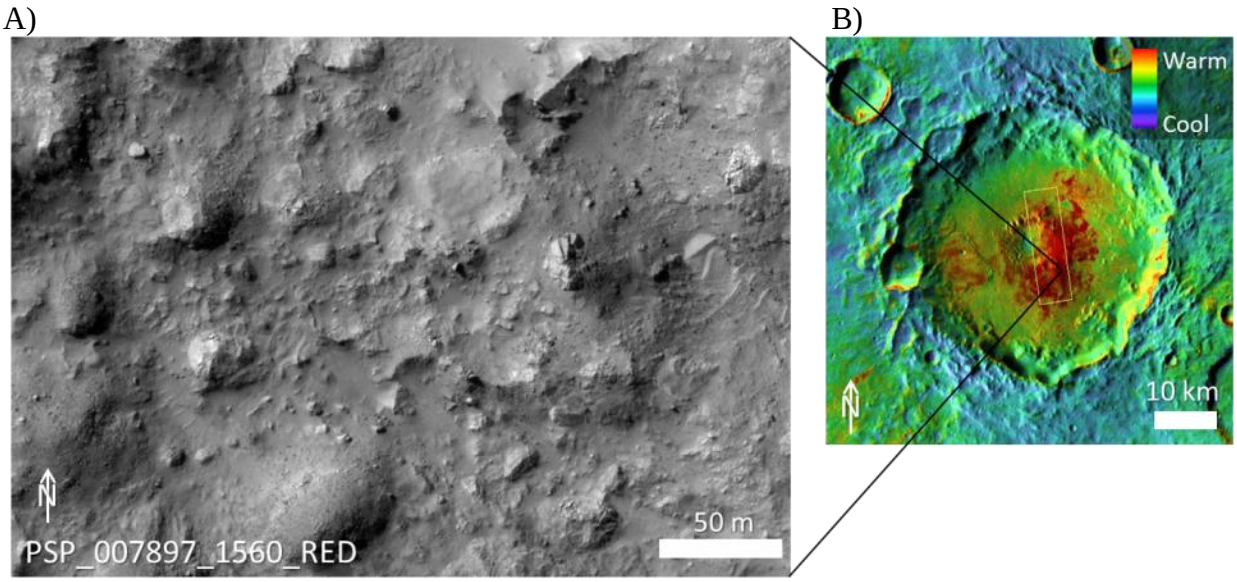

Fig. 9: A) HiRISE image showing large blocks near a central pit crater at 23.8°S, 126.8°E. B) THEMIS nighttime IR (color) over daytime IR (shading) context image showing warm material inferred as being blocky and confirmed by the HiRISE image. Black lines indicate location of A. Yellow box in B indicates footprint of HiRISE image.

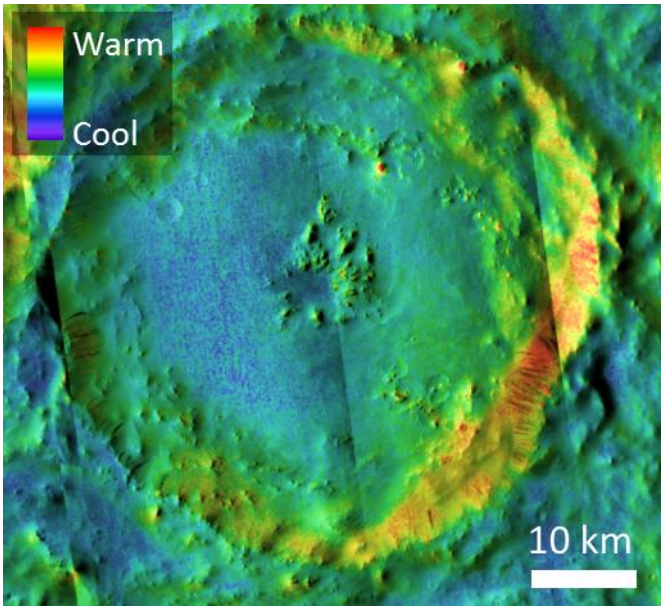

Fig. 10: THEMIS nighttime IR (color) over CTX visible (shading) image showing a central pit crater at 10.9°N, 50.8°E. We interpret the lack of a warm thermal signature surrounding the central pit here as being due to mantling by fine-grained dust and/or sand.

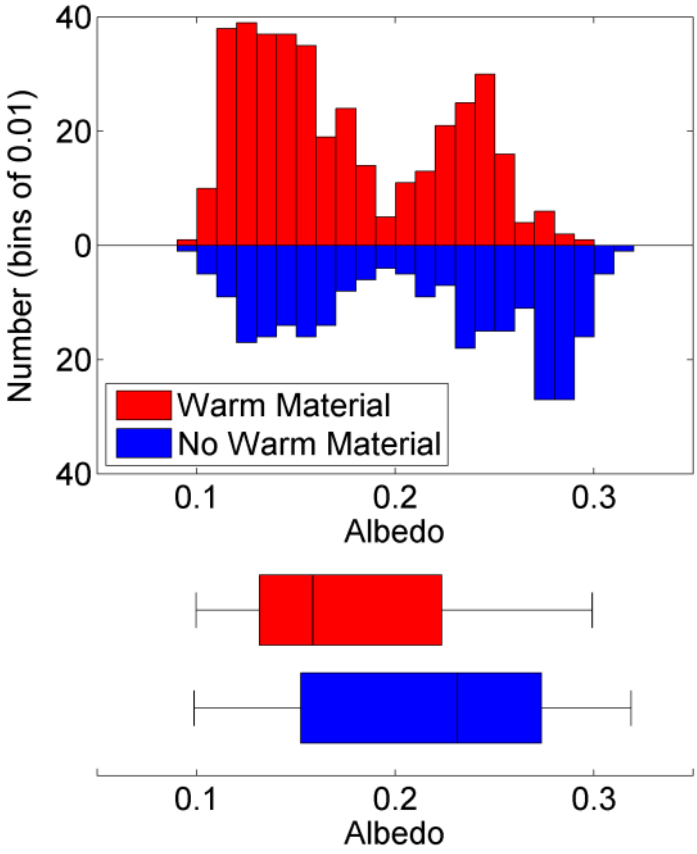

Fig. 11: Histogram and box-and-whisker plot of central pit craters exhibiting warm THEMIS night-time temperatures (red) and those without warm temperatures (blue) as a function of regional albedo from TES [Christensen *et al*., 2001].

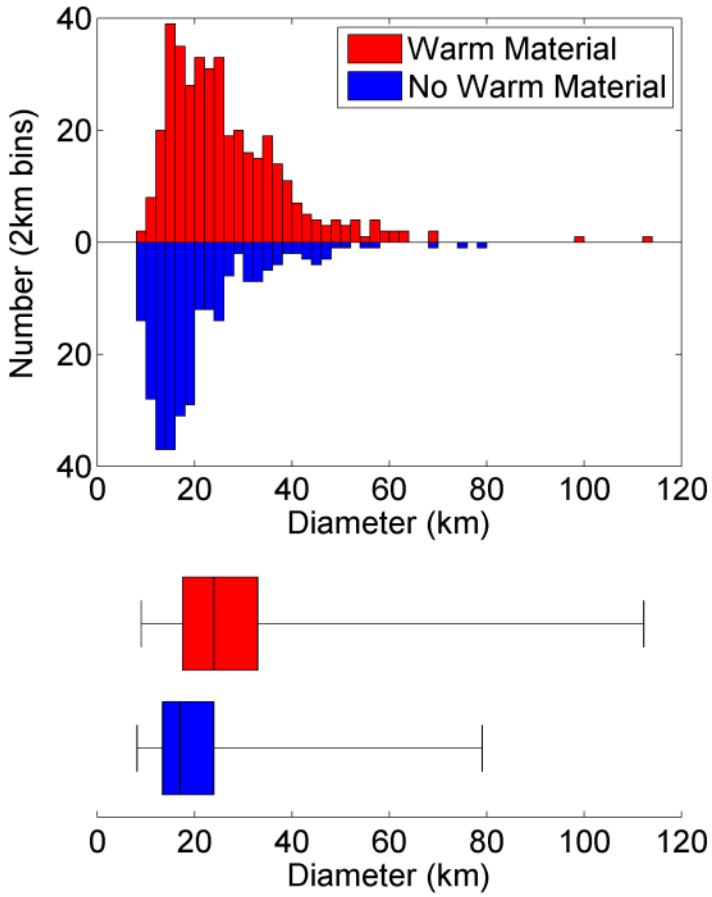

Fig. 12: Histogram and box-and-whisker plot of craters containing central pits exhibiting warm THEMIS night-time temperatures (red) and those without warm temperatures (blue) as functions of the parent crater diameter.

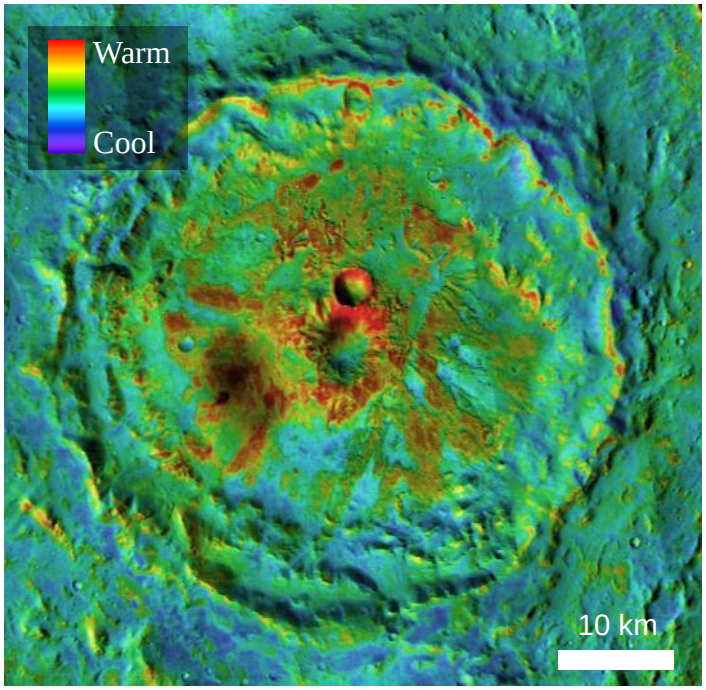

Fig. 13: THEMIS nighttime IR (color) over CTX visible (shading) image showing dispersed lava or perhaps impact melt flows on the floor of an impact crater containing a central pit (28.5°N, 83.4°W).

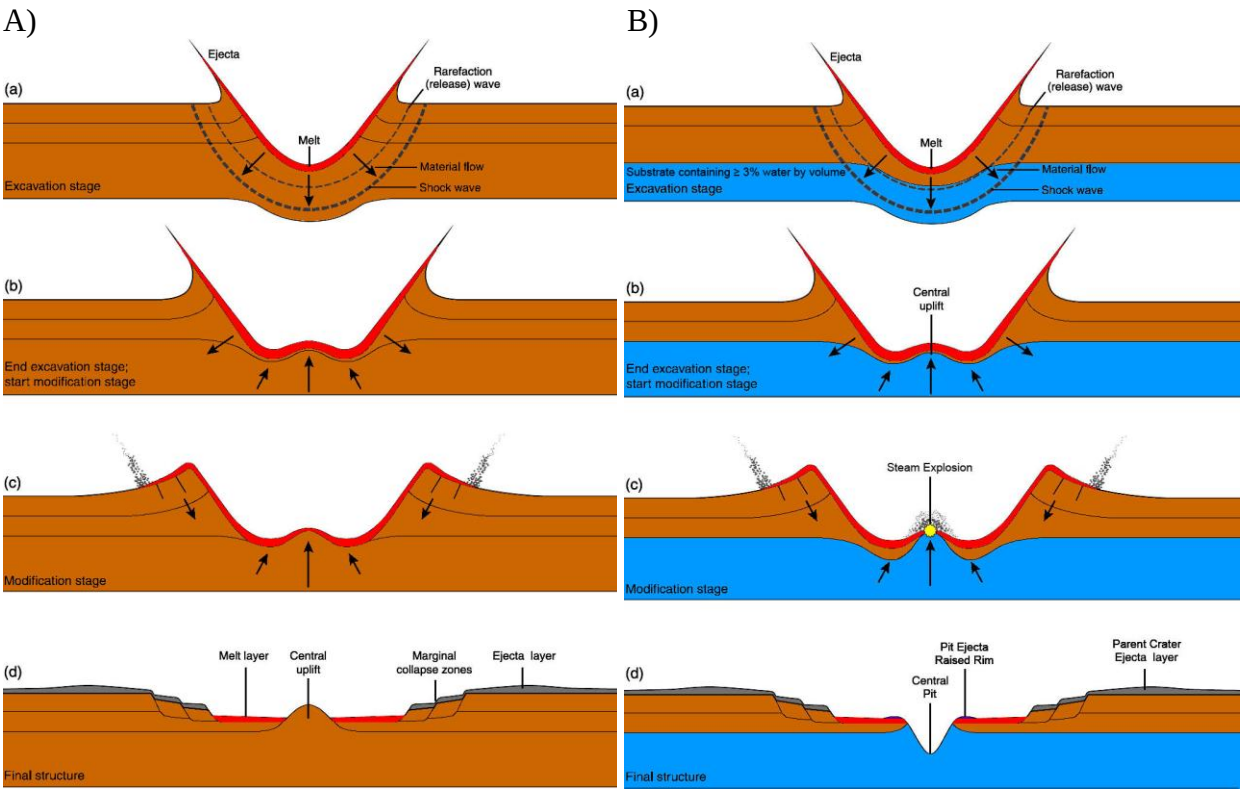

Fig. 14: Schematic cartoons illustrating steps in complex crater formation resulting in: A) a classical central peak [modified from French, 1998], and B) our proposed new "uplift contact model" for Martian central pit crater formation.